Synchrotron Radiation as a Foreground for the CMB (Physics 239 - Final Paper)

Lindsay Ng Lowry

December 5, 2016

Abstract

Radiation generated by the radial acceleration of relativistic charged particles about magnetic field lines is known as synchrotron emission. Considering an ensemble of charged particles, the intensity of this type of radiation varies with frequency in a way that depends on the particles' energy distribution, and generally decreases at higher frequencies. Additionally, emission from synchrotron sources can be polarized, where the degree of polarization is also related to the energy distribution of the particles. One of the motivations for studying synchrotron radiation in astrophysics is its characterization as a foreground as electrons interact with galactic magnetic fields. This is of particular importance to polarization-sensitive surveys of the cosmic microwave background (CMB). We explore the mechanisms that generate synchrotron emission as foreground sources and how to account for these sources in the context of CMB experiments.

1 Introduction

Charged particles in the universe are often accelerated by magnetic fields and thus will radiate. The simplest form of this radiation is called cyclotron radiation, which occurs when charged particles moving at non-relativistic speeds are accelerated about magnetic field lines. In this case, the particle begins moving in a circular motion and an observer will see radiation at a single frequency corresponding to this frequency of rotation. However, the emitted radiation becomes more complex as the velocities of the charged particles increase. Doppler effects become important and thus higher harmonics of the rotation frequency begin to contribute to the observed spectrum. Velocities approaching the speed of light, c, and broadening mechanisms such as nonuniform magnetic field strength produce polarized radiation with a continuous spectrum. This is what is known as synchrotron radiation.

The presence of magnetic fields and cosmic ray electrons within our galaxy creates synchrotron radiation observable on Earth. Cosmic ray electrons with energies on the order of GeV interact with galactic magnetic fields with strengths of a few microGauss to produce synchrotron radiation peaking in the MHz-GHz range [1], [2]. This frequency range overlaps with the lower end of that related to studies of the cosmic microwave background (CMB). Measuring the CMB is an active area of research with the primary aim of unveiling properties of the early universe and characterizing stages in its evolution. In order to make justifiable cosmological predictions based on these measurements, it is crucial to accurately filter out any microwave signal arising from sources other than the CMB.

Modeling synchrotron emission from the galaxy involves an understanding of the fundamental processes, simulations based on those processes and independently obtained estimates of galactic parameters, and observed data sets for comparison. In Section 2 we will derive some observable properties of synchrotron radiation. In Section 3 we will then look at the way this radiative process is modeled and its application to measurements of the CMB.

2 Properties of Synchrotron Radiation

To produce accurate foreground models of synchrotron radiation we must first understand the total power emitted and then look more closely to derive how this power is distributed as a function of frequency.

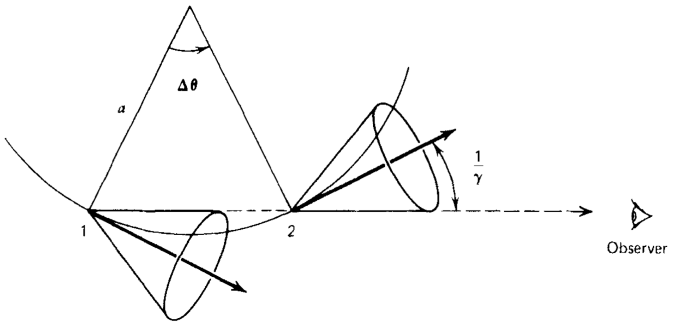

Figure 1: Relativistic particle and its cone of radiation at two points, 1 and 2, along its trajectory, from Rybicki and Lightman [3]. Due to the relativistic nature of the particle, the radiation is confined to a cone centered about the particle's velocity, such that the depicted observer is only able to receive radiation emitted while the particle is between points 1 and 2.

2.1 Particle Trajectory and Total Power

The relativistic force equations for a charge, q, moving at velocity $\vec{v}$ under the influence of a magnetic field, $\vec{B}$, are given by

$$\frac{d}{dt}(\gamma mc^2) = q(\vec{v} \cdot \vec{E}). \tag{1}$$

$$\frac{d}{dt}(\gamma m\vec{v}) = \frac{q}{c}(\vec{v} \times \vec{B}), \tag{2}$$

Since $\vec{E} = 0$, Equation 1 implies a constant γ. Thus the magnitude of the particle's velocity, v, does not change as it interacts with the magnetic field. Decomposing Equation 2 into velocity components parallel and perpendicular to the magnetic field, $v_{\parallel}$ and $\vec{v_{\perp}}$, then shows that

$$v_{\parallel} = const \quad \text{and} \quad |\vec{v_{\perp}}| = const. \tag{3}$$

Thus, the trajectory of the particle is helical motion along $\vec{B}$. We define the frequency of rotation as

$$\omega_B \equiv \frac{qB}{\gamma mc}, \tag{4}$$

where $B \equiv |\vec{B}|$.

Equation 2 also gives us information about the particle's acceleration both parallel and perpendicular to the magnetic field. Plugging these results into the relativistic Larmor formula and defining $\beta_{\perp} \equiv v_{\perp}/c$ yields a total emitted power of

$$P_{\text{total}} = \left(\frac{2}{3}\right)^2 \frac{q^4\beta^2\gamma^2B^2}{m^2c^3}, \tag{5}$$

where we have assumed an isotropic distribution of particle velocities and averaged over all angles of $\vec{v}$ with respect to $\vec{B}$ [3].

2.2 Spectrum and Polarization

Due to relativistic beaming effects it is clear that the observed radiation from synchrotron sources will differ from that produced by cyclotron sources despite the similarities between the two mechanisms. The radiation emitted by a relativistic electron is concentrated in the direction of the particle's motion, whereas that of a nonrelativistic electron is more isotropic. Thus, an observer will only see synchrotron radiation when the particle is at particular points along its trajectory, as shown in Figure 1. The emitted radiation is seen in pulses rather than a continuous sine wave as in cyclotron radiation, and the resulting spectrum is more complex.

The spectrum for a moving charge is given by

$$\frac{dW}{d\omega d\Omega} = \frac{q^2\omega^2}{4\pi^2 c}\left|\int \left[\hat{n} \times (\hat{n} \times \vec{\beta})\right] \exp i\omega\left[t' - \frac{\hat{n} \cdot \vec{r}(t')}{c}\right] dt'\right|^2, \tag{6}$$

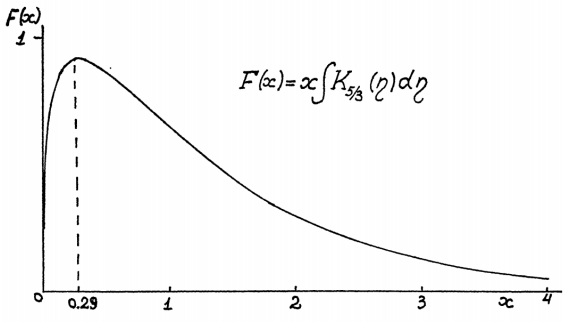

Figure 2: Plot of $F(x)$, depicting the frequency dependence of the total power emitted [4]. The spectrum peaks at $\omega = 0.29\omega_c$.

where $\hat{n}$ is the unit vector pointing from the particle to the observer and $\vec{r}(t)$ describes the particle's path. The first term in the integral contains two terms, one proportional to each polarization state. We can therefore evaluate the spectrum for each polarization state separately. Assuming $v \approx c$ and integrating over solid angle, we divide over the orbital period $T = 2\pi/\omega_B$ to find

$$P_{\parallel}(\omega) = \frac{\sqrt{3}q^3 B \sin\alpha}{4\pi mc^2}[F(x) + G(x)], \tag{7}$$

$$P_{\perp}(\omega) = \frac{\sqrt{3}q^3 B \sin\alpha}{4\pi mc^2}[F(x) - G(x)], \tag{8}$$

where

$$x \equiv \frac{\omega}{\omega_c}, \quad \omega_c \equiv \frac{3\gamma^2 qB\sin\alpha}{2mc} \tag{9}$$

and

$$F(x) \equiv x\int_x^{\infty} \mathcal{K}_{5/3}(\eta)d\eta, \quad G(x) \equiv x\mathcal{K}_{2/3}(x) \tag{10}$$

where $\mathcal{K}$ denotes the modified Bessel function [3]. Total power is thus proportional to $F(x)$, plotted in Figure 2. The details involved in this derivation can be found in Rybicki and Lightman [3] and Ginzburg and Syrovatskii [4].

3 Modeling Synchrotron Radiation

In order to obtain useful information about astrophysical synchrotron radiation, it is necessary to compare the properties described above to observational data and create a model that can be used in other applications. The derived equations simplify slightly if assuming a power law distribution of electron energies, $N(\gamma)d\gamma = C\gamma^{-p}d\gamma$. In this case, the spectrum of total synchrotron radiation also obeys a power law [3] given by

$$P_{\text{tot}}(\omega) = \frac{\sqrt{3}q^3 CB\sin\alpha}{2\pi mc^2(p+1)}\Gamma\left(\frac{p}{4}+\frac{19}{12}\right)\Gamma\left(\frac{p}{4}-\frac{1}{12}\right)\left(\frac{mc\omega}{3qB\sin\alpha}\right)^{-\frac{p-1}{2}}, \tag{11}$$

and the degree of linear polarization is

$$\Pi = \frac{p+1}{p+\frac{7}{3}}. \tag{12}$$

The assumption of a power law distribution of electrons when studying synchrotron radiation in the galaxy is justified both by the nature of the mechanisms creating cosmic ray electrons in the galaxy [5], observations of the electrons themselves [6], and direct observations of synchrotron radiation [7].

The idea behind synchrotron modeling for CMB experiments is to take a polarized map of the sky at a frequency dominated by synchrotron foreground emission as a template, determine the

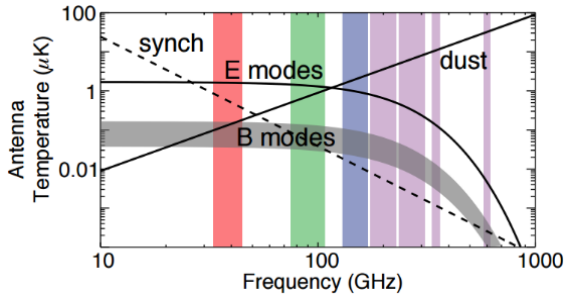

Figure 3: Schematic diagram showing CMB foregrounds and signals with their relative intensities as a function of frequency [12]. Colored bands indicated the frequency bands of CLASS and PIPER (two CMB experiments). Synchrotron emission is dominant at lower frequencies, while emission from dust dominates at higher frequencies.

typical spectral index β[1] of galactic synchrotron emission, and use this value of β to scale the template map up to show the expected synchrotron emission in the desired frequency band. This scaled map then defines the model and can be subtracted from CMB observations. Typical values of β range from about -3.3 to -2.6 [9], [10], [11]. The template maps chosen generally come from full-sky observations taken in frequency bands lower than those targeted for CMB science as this is where synchrotron radiation dominates. A similar technique is used for modeling foreground radiation from dust which is dominant to the CMB signal at higher frequencies (hundreds of GHz). A schematic diagram depicting the typical frequency dependence of these foreground sources compared to the CMB signal is shown in Figure 3.

3.1 Difficulties with Synchrotron Modeling

As with any type of physical model, models of galactic foreground synchrotron emission are imperfect. Limitations are largely due to the finite resolution and amount of sky data currently available. Usefulness of the models to a specific experiment is also then limited by the ability to model that experiment's instrumental effects. In this section we will discuss some of the main difficulties associated with modeling synchrotron emission for the CMB, based on two recently developed applications for modeling, described in [9] and [8].

3.1.1 Polarized Data

One issue with modeling synchrotron emission for polarized CMB measurements is the lack of polarized data. Though multiple satellites have obtained data across the full sky at frequencies useful for synchrotron emission, most data sets only map the total intensity. Current ground-based CMB experiments are hoping to detect a polarized signal which they obtain by differencing the received signals from two orthogonal polarized detectors, and thus the nonzero degree of linear polarization from synchrotron emission and accurate templates of polarized emission are important.

This problem has been substantially alleviated by the recent publication of Planck polarized foreground data at frequencies down to 30 GHz [13], [9]. However, despite this improvement, constructing templates from these maps remains a nontrivial task as smoothing the map is necessary to remove nonphysical artifacts arising from Planck's pixelization. This smoothing in turn worsens the resolution, removing power at small angular scales. Models can compensate for this loss by extrapolating the power spectra and using this information to make random realizations of the map to add at small scales. This technique helps to regain features at high-ℓ, but relies on assumptions about the shape of the spectra [9], [8].

Finally, lack of polarization data of the galaxy and its magnetic field at multiple frequencies drives models to rely on the assumption that the spectral index is the same for polarized and unpolarized data, resulting in models that are likely oversimplified [8].

[1] In CMB experiments, β is typically defined, up to a sign, such that $I_\nu \propto \nu^\beta$, where I_ν is given in antenna temperature units and thus $\beta = -\frac{(p+3)}{2}$ for an electron energy distribution described above [8].

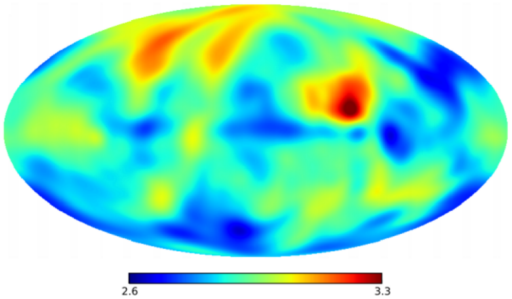

Figure 4: Map depicting the spatial variation of β, generated from maps at radio frequencies and from Planck. This map is used in the model described in [9].

3.1.2 Spatial Dependence of β

Though evidence suggests the distribution of electrons does in fact adhere to a power law, this assumption is not always valid on large scales as the spectral index is seen to vary slightly with position on the sky. Using data from Planck, the best-fit spectral index is $\beta = -3.10$ assuming β is constant over the full sky [9]. However, improved fits can be obtained by assuming a continuous change in spectral index with Galactic latitude [8], or by dividing the sky into multiple smaller regions and fitting a spectral index in each [9], as shown in Figure 4. The former method likely results in a still oversimplified model that does not account for small-scale changes in the galaxy, while difficulties with the latter method arise from requiring more data which necessitate combining multiple data sets. If these sets of data reference different frequency bands the combination may cause discrepancies due to phenomena described in the next section.

3.1.3 Frequency Dependence of β

Along with spatial variations, it has been suggested that β can vary with frequency which thus affects the scaling of the template map. Both models referenced here include this "curvature" of β as an option for the user. The curvature is included in the model by replacing β by

$$\beta' \equiv \beta + C \log(\nu/\nu_{\text{piv}}). \tag{13}$$

C indicates the degree to which the spectral index flattens or steepens and ν_{piv} is the frequency at which this change occurs [9], [8]. Again, though the inclusion of this effect makes the model more sophisticated, it requires analysis of multiple data sets, specifically at several frequencies.

3.2 An Example: The Cosmology Large Angular Scale Surveyor

One ground-based CMB experiment that contains a telescope specifically designed to target this foreground emission from synchrotron sources is the Cosmology Large Angular Scale Surveyor (CLASS). CLASS will be a four-telescope array, the first of which achieved first light in May 2016 and has a frequency band centered at 38 GHz [14]. Data from this telescope will be used to clean the higher-frequency data of synchrotron radiation. A similar telescope with high-frequency channels will be used to clean for dust.

Watts et al. 2015 [10] describes foreground simulations that have been performed in preparation for CLASS. Modeling techniques similar to those discussed above are used with Planck data to simulate the synchrotron signal CLASS will measure in order to demonstrate CLASS's ability to recover CMB information in the future. The hope is that data from all four telescopes will allow CLASS to model foregrounds and clean CMB data with minimal external data.

4 Conclusion

Polarized synchrotron emission from the galaxy contaminates current observations of the CMB. To obtain clean data of the CMB, synchrotron emission must be modeled accurately. Though polarized synchrotron models have recently benefited from the release of data from the Planck satellite, issues arising from the complex distribution of this radiation remain. Ongoing and future CMB experiments such as CLASS aim to further improve these models and cleaning techniques.

References

[1] Di Bernardo, G., Grasso, D., Evoli, C., & Gaggero, D. 2015, ASTRA Proceedings, 2, 21

[2] Strong, A. W., Orlando, E., & Jaffe, T. R. 2011, *Astronomy and Astrophysics*, 534, A54

[3] Rybicki, G. B., & Lightman, A. P. 1979, New York, Wiley-Interscience, 1979. 393 p.

[4] Ginzburg, V. L., & Syrovatskii, S. I. 1965, *Annual Review of Astronomy and Astrophysics*, 3, 297

[5] Condon, J. & Ransom, S., *Essential Radio Astronomy*. Princeton: Princeton University Press. 2016.

[6] Casadei, D., & Bindi, V. 2004, ApJ, 612, 262

[7] Platania, P., Bensadoun, M., Bersanelli, M., et al. 1998, ApJ, 505, 473

[8] Thorne, B., Dunkley, J., Alonso, D., & Naess, S. 2016, arXiv:1608.02841

[9] Hervías-Caimapo, C., Bonaldi, A., & Brown, M. L. 2016, *MNRAS*, 462, 2063

[10] Watts, Duncan J., et al. "Measuring the Largest Angular Scale CMB B-mode Polarization with Galactic Foregrounds on a Cut Sky." *The Astrophysical Journal* 814.2 (2015): 103.

[11] Shaver, P. A., Windhorst, R. A., Madau, P., & de Bruyn, A. G. 1999, *Astronomy and Astrophysics*, 345, 380

[12] Eimer, J. "Cosmology Large Angular Scale Surveyor: CLASS." CAS Seminar, 26 April 2012. http://sites.krieger.jhu.edu/class/files/2013/09/CLASS_overview.pdf

[13] Planck Collaboration, Adam, R., Ade, P. A. R., et al. 2016, *Astronomy and Astrophysics*, 594, A10

[14] Harrington, K., Marriage, T., Ali, A., et al. 2016, arXiv:1608.08234